

See discussions, stats, and author profiles for this publication at: <https://www.researchgate.net/publication/231235369>

# Preparation and Characterization of a Highly Stable Pillared Clay: GaAl<sub>12</sub>-Pillared Rectorite

ARTICLE *in* CHEMISTRY OF MATERIALS · JULY 1995

Impact Factor: 8.35 · DOI: 10.1021/cm00055a017

---

CITATIONS

18

---

READS

9

## 2 AUTHORS:



[Stephen A. Bagshaw](#)

Independent Researcher

35 PUBLICATIONS 2,193 CITATIONS

SEE PROFILE



[Ralph P Cooney](#)

University of Auckland

144 PUBLICATIONS 2,900 CITATIONS

SEE PROFILE

# Preparation and Characterization of a Highly Stable Pillared Clay: GaAl<sub>12</sub>-Pillared Rectorite

Stephen A. Bagshaw<sup>†</sup> and Ralph P. Cooney\*

Department of Chemistry, University of Auckland, Private Bag 92019, Auckland, New Zealand

Received February 14, 1995. Revised Manuscript Received April 7, 1995<sup>®</sup>

The preparation, thermal stabilities and surface acid characteristics of a novel microporous GaAl<sub>12</sub>-pillared rectorite have been studied. GaAl<sub>12</sub>-pillared rectorites with different pillar concentrations ranging from 2.0 to 6.0 mmol of GaAl<sub>12</sub> g<sup>-1</sup> of clay, are reported. The GaAl<sub>12</sub>-pillared rectorite with pillar loading of 6.0 mmol (42 mequiv) GaAl<sub>12</sub> g<sup>-1</sup> of clay, exhibits outstanding thermal stability, maintaining a strongly ordered gallery spacing of 1.00 nm and therefore microporosity, after heating in air at 973 K. Analysis of the IR spectra of adsorbed pyridine revealed both Lewis and Brönsted acid sites similar to those observed for Al<sub>13</sub>-pillared rectorite. Increasing the concentration of pillars from 2.0 to 6.0 mmol GaAl<sub>12</sub> g<sup>-1</sup> of clay, produces materials that possess both greater thermal stability and more abundant acidity. This novel catalytic material represents an overall improvement in both the thermal stability and acid strength of existing alumina-based pillared montmorillonites and rectorites.

## Introduction

A new class of porous solid-acid catalysts, where robust inorganic polyoxo cations are intercalated between the layers of aluminosilicate hosts, the so-called pillar interlayered clays (PILCs), has recently received considerable attention in the search for new materials that possess catalytic properties which will compliment existing molecular sieve technologies.<sup>1–3</sup> Two major hurdles in the development of PILC materials to date have been low thermal and hydrothermal stabilities leading to collapse of the pillared structure under catalytic and regeneration conditions and low Brönsted/Lewis (B/L) acid ratios, resulting in high coke make during hydrocracking and other important catalytic reactions.<sup>1–3</sup>

An important development in the preparation of thermally stable PILCs came with the preparation of [AlO<sub>4</sub>Al<sub>12</sub>(OH)<sub>24</sub>(H<sub>2</sub>O)<sub>12</sub>]<sup>7+</sup> or Al<sub>13</sub>-pillared rectorite.<sup>4</sup> This material retained its pillared structure under steam treatment at 1073 K and was resistant to heavy-metal (1000 ppm V) poisoning. The surface acidity of Al<sub>13</sub>-pillared rectorite has been shown to possess higher Brönsted/Lewis acid ratios than Al<sub>13</sub>-pillared montmorillonite.<sup>5</sup> This was reported to be due to the presence of tetrahedral substitution in the rectorite tetrahedral layers that allowed the ready formation of strong layer-pillar linkages that are in turn converted into protonic acid sites. Additionally, the greater thermal stability

demonstrated by this material, allowed access by adsorbate and reactant molecules to the intergallery space at higher temperatures than Al<sub>13</sub>-pillared montmorillonite.<sup>1,4</sup> A second major advance was the preparation of the [GaO<sub>4</sub>Al<sub>12</sub>(OH)<sub>24</sub>(H<sub>2</sub>O)<sub>12</sub>]<sup>7+</sup> or GaAl<sub>12</sub> mixed-metal polyoxo cation and subsequent intercalation of this species<sup>6,7</sup> into montmorillonite. In this species, the central tetrahedral Al<sup>3+</sup> ion of the Al<sub>13</sub> cation, the structure of which is described as that of the Baker-Figgis  $\epsilon$  isomer<sup>8</sup> of the Keggin structure, is replaced with a Ga<sup>3+</sup> ion. It was proposed that the slightly larger ionic radius of the Ga<sup>3+</sup> ion makes the GaAl<sub>12</sub> structure more symmetric than the parent aluminium oligomer.<sup>9–11</sup> The consequences of this are that the GaAl<sub>12</sub> cation is thermodynamically favored over both the Al<sub>13</sub> and the Ga<sub>13</sub> species and that it is considerably more thermally stable than either of those two oligocations. Intercalation of the GaAl<sub>12</sub> species into montmorillonite clay produced<sup>6</sup> a PILC stable to prolonged calcination at at least 873 K.

Infrared (IR) spectroscopic studies of adsorbed pyridine have been widely used in the study of the surface acidity of solid acid catalysts,<sup>12–14</sup> including pillared clays.<sup>5,15</sup> The current literature maintains that the acidity of metal oxide pillared clays is primarily of the Lewis type, with a significant Brönsted contribution and located principally on the surfaces of the pillars themselves. The Brönsted/Lewis acid ratios of PILCs can be

\* To whom correspondence should be addressed.

<sup>†</sup> Current address: Department of Chemistry and Center for Fundamental Materials Research, Michigan State University, East Lansing, MI 48824.

<sup>®</sup> Abstract published in *Advance ACS Abstracts*, May 15, 1995.

(1) Burch, R., Ed. *Catal. Today*, **1988**, 2, 1.

(2) Pinnavaia, T. J. In *Chemical Interactions in Organic and Inorganic Constrained Systems*; Setton, R., Ed.; Reidel: Amsterdam, 1986; p 151.

(3) Figueras, F. *Catal. Rev. Sci. Eng.* **1988**, 30, 457.

(4) Guan, J.; Min, E.; Yu, Z. *Proc. 9th Int. Conf. Catal.*, Calgary **1988**, 104.

(5) Bagshaw, S. A.; Cooney, R. P. *Chem. Mater.* **1993**, 5, 1101.

(6) Bradley, S. M.; Kydd, R. A. *Catal. Lett.* **1991**, 8, 185.

(7) González, F.; Pesquera, C.; Blanco, C.; Mendioroz, S. *Inorg. Chem.* **1992**, 31, 31.

(8) Baker, L. C. W.; Figgis, J. S. *J. Am. Chem. Soc.* **1970**, 92, 3794.

(9) Tang, X.; Xu, W.-Q.; Shen, Y.-F.; Suib, S. L. *Chem. Mater.* **1994**, 7, 102.

(10) Bradley, S. M.; Kydd, R. A.; Yamdagni, R. *Magn. Reson. Chem.* **1990**, 28, 746.

(11) Bradley, S. M.; Kydd, R. A.; Fyfe, C. A. *Inorg. Chem.* **1992**, 31, 1181.

(12) Parry, E. P. *J. Catal.* **1963**, 2, 371.

(13) Little, L. H. *Infrared Spectra of Adsorbed Species*; Academic Press: London, 1966.

(14) Ward, J. W. *J. Catal.* **1968**, 11, 271.

(15) Ming-Yuan, H.; Zhonghui, L.; Enze, M. *Catal. Today* **1988**, 2, 321.

tuned somewhat by judicious choice of both the pillaring species and the parent layered host. The lowest B/L ratio is observed with titania pillars,<sup>5</sup> while the highest is produced by alumino-silica pillars<sup>16</sup> and fluorinated layered hosts.<sup>5,17</sup> The overall acidity of GaAl<sub>12</sub>-pillared montmorillonite was reported to be stronger than Al<sub>13</sub>-pillared montmorillonite.<sup>6</sup> This was attributed to the improved thermal stability of the GaAl<sub>12</sub>-pillared montmorillonite which allowed access to the interlayer gallery space and hence surface acid sites, to be maintained to temperatures (i.e., at least 873 K) greater than those previously reported.

The aim of the current investigation was to combine the high thermal stabilities of both the layered structure of rectorite and the GaAl<sub>12</sub> oligocation, with proven synthetic techniques, in the preparation of a new more stable PILC material and to investigate the thermal stability and surface acid characteristics of this material.

## Experimental Section

**Synthesis.** Arkansas rectorite (RAR-1) was obtained from the Source Clays Repository, University of Missouri. The clay was purified by sieving and aqueous dispersion techniques, then converted into the Na<sup>+</sup> form by exchange with excess 1.0 mol L<sup>-1</sup> NaCl solution. The Na<sup>+</sup>-rectorite was then dialyzed to remove Ca<sup>2+</sup> and Cl<sup>-</sup> ions from the suspension. A GaAl<sub>12</sub> solution was prepared using a slightly modified version of the method described by Bradley et al.<sup>6</sup> Al(H<sub>2</sub>O)<sub>6</sub><sup>3+</sup> solution (0.2 mol L<sup>-1</sup>) was prepared from Strem Chemicals AlCl<sub>3</sub>·6H<sub>2</sub>O. An aqueous Ga<sup>3+</sup> solution was prepared by dissolving 99.999% pure PROLABO Ga metal in a minimum of concentrated HCl, followed by dilution with deionized water, to produce a solution, most likely containing Ga(H<sub>2</sub>O)<sub>6</sub><sup>3+</sup>, 0.203 mol L<sup>-1</sup> in Ga. Portions of each of the two solutions were vigorously stirred together in a 1:12 Ga:Al ratio. This solution was then rapidly hydrolyzed, under stirring, to an OH:M<sup>3+</sup> partial hydrolysis ratio (*r*) of 2.2 by the dropwise addition of 0.2 mol L<sup>-1</sup> NaOH solution at room temperature. The solution was then heated under reflux at 333 K for 16 h in order to convert any Al<sub>13</sub> or Ga<sub>13</sub> cations that may have formed during the hydrolysis, into GaAl<sub>12</sub> species.<sup>10</sup>

The GaAl<sub>12</sub>-pillared rectorite samples were prepared using the ion-exchange and dialysis techniques previously described by Bagshaw and Cooney.<sup>5</sup> GaAl<sub>12</sub>-exchanged clays with three different pillar concentrations were prepared by the dropwise addition of 2.0 mmol (14 mequiv), 4.0 mmol (28 mequiv), and 6.0 mmol (42 mequiv) of GaAl<sub>12</sub> solution/g of clay, to aliquots of the vigorously stirred Na<sup>+</sup>-rectorite suspension of known mass per volume. After reaction for 16 h, each sample was transferred to dialysis tubing and dialyzed in doubly distilled water for 4 days to remove Na<sup>+</sup> and Cl<sup>-</sup>. The dialysis water was changed each day until the water-tested Cl<sup>-</sup> free by the AgNO<sub>3</sub> test. The GaAl<sub>12</sub>-exchanged clays were subsequently separated from suspension by centrifugation and dried in air at 333 K. The pillared clays thereby prepared are henceforth assigned the descriptors; GaAl-*R N*, where *R* stands for rectorite and *N* is the nominal number of moles of GaAl<sub>12</sub> pillars in mmol of M<sup>3+</sup> g<sup>-1</sup> of clay that was added to the parent clay.

**Characterization.** *NMR Spectra.* <sup>27</sup>Al and <sup>71</sup>Ga NMR spectroscopic analyses of the GaAl<sub>12</sub> pillaring solution were performed on a Bruker AM400/Aspect 3000 spectrometer at room temperature operating at 104.263 MHz for <sup>27</sup>Al and 122.028 MHz for <sup>71</sup>Ga. Chemical shifts were referenced to 0.1 mol L<sup>-1</sup> Al(NO<sub>3</sub>)<sub>3</sub> and Ga(NO<sub>3</sub>)<sub>3</sub> respectively in H<sub>2</sub>O/D<sub>2</sub>O.

*X-ray Diffraction Patterns.* Preferred orientation X-ray diffraction (XRD) slides of each Cl<sup>-</sup> free GaAl<sub>12</sub>-exchanged clay

sample were prepared before drying. These slides were dried then subjected to heat treatment by heating at approximately 5 K min<sup>-1</sup> in air, to temperatures ranging from 298 to 973 K and maintaining the desired temperature for 2 h. XRD patterns were obtained with a Philips PW1050 goniometer employing a Cu Kα X-ray source connected to Seitronics Sieray 112 computer. Because there is little useful information to be observed at higher angles, the XRD patterns obtained from 2 to 20° 2θ are displayed, after conversion to the corresponding *d*<sub>001</sub> values, from 2 to 10° 2θ.

*Surface Area Measurements.* N<sub>2</sub> adsorption/desorption isotherms of PILCs calcined at 423 and 773 K were obtained with a Coulter Omnisorb 360CX sorptometer by adsorption of N<sub>2</sub> at 70 K. Samples were outgassed at 423 K under approximately 0.01 N m<sup>-2</sup> vacuum for 16 h prior to analysis. The BET equation was used to determine the surface areas from analysis of the adsorption isotherms.

*Fourier Transform Infrared Spectroscopy.* The surface acidities of the GaAl<sub>12</sub> PILCs were studied by IR spectroscopy of adsorbed pyridine. PILC samples were prepared as self-supporting wafers (mass 10–15 mg) and placed in a glass/quartz in situ IR and Raman cell which allowed simultaneous and identical treatment of three samples. Each GaAl-R sample was activated at 773 K in O<sub>2</sub> (1 × 10<sup>5</sup> N m<sup>-2</sup>) for 5 h, then degassed at approximately 0.01 N m<sup>-2</sup> at the same temperature for 2 h. The samples were cooled to room temperature and exposed to pyridine vapor for 12 h to allow for complete diffusion of the pyridine vapor into the pore structure. Excess pyridine was then evacuated at room temperature for 2 h. This was followed by stepwise desorption of the adsorbed pyridine at increasing temperatures for 2 h. IR spectra were obtained at room temperature after each desorption step by the coaddition of 500 scans at 2.0 cm<sup>-1</sup> resolution with a Digilab FTS-60 FTIR spectrometer equipped with a deuterated triglycine sulfate (DTGS) detector and N<sub>2</sub> gas compartment purge to remove the contributions to the recorded spectra arising from the background gases. This method allowed for greater accuracy from the spectral background ratioing software.

## Results and Discussion

**NMR.** <sup>71</sup>Ga NMR spectra (Figure 1A) reveal only one resonance, arising from Ga in a symmetrical tetrahedral coordination environment at a chemical shift of δ 137.5. No signal from six-coordinate Ga (δ 0.0) was observed, indicating that all the Ga(H<sub>2</sub>O)<sub>6</sub><sup>3+</sup> had been hydrolyzed. The <sup>27</sup>Al NMR (Figure 1B) spectra show the opposite situation, where only a very weak and broad resonance that may be assigned to Al in tetrahedral coordination (δ 63) was observed. The resonance at (δ 0.0) is assigned to Al in octahedral coordination (Al(H<sub>2</sub>O)<sub>6</sub><sup>3+</sup>), indicating the presence of unreacted Al(H<sub>2</sub>O)<sub>6</sub><sup>3+</sup> cations. These results suggest that only GaAl<sub>12</sub><sup>7+</sup> and Al(H<sub>2</sub>O)<sub>3</sub><sup>6+</sup> species are present in the pillaring solution.<sup>7</sup> The multinuclear NMR technique for characterization of these species is now well established, and while it is possible that not all of the Ga or Al is observed in the NMR spectra owing to quadrupolar or exchange effects, the results given here are consistent with both the existing literature<sup>6,7,10</sup> and the results discussed below.

**Thermal Stability of GaAl<sub>12</sub> Pillared Rectorite.** XRD patterns obtained for the various GaAl<sub>12</sub>-pillared rectorites (Figure 2), display the response of the *d*<sub>001</sub> basal spacing and therefore the gallery height, to heating in air at increasing temperatures (Table 1). The *d*<sub>001</sub> basal spacing minus the combined width of one 2:1 smectite layer plus the two nonswelling illite layers (approximately 1.90 nm) gives the gallery height. Heating of the GaAl-R2 sample at 473 K (Figure 2A(b))

(16) Lou, G.; Huang, P. M. *Clays Clay Miner.* **1993**, *41*, 38.

(17) Butruille, J.-R.; Michot, L. J.; Barrés, O.; Pinnavaia, T. J. *J. Catal.* **1993**, *139*, 664.

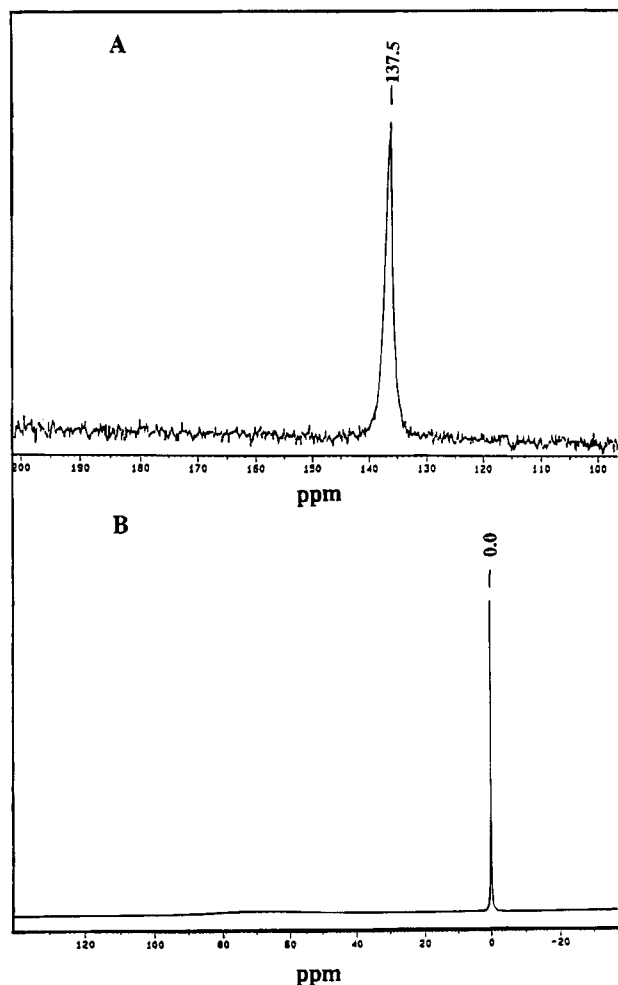


**Figure 1.** Solution NMR spectra of  $\text{GaAl}_{12}$  solution prepared by mixing  $\text{Ga}^{3+}$  and  $\text{Al}^{3+}$  solutions in 1:12 ratio followed by rapid hydrolysis to  $\text{OH}/\text{M}^{3+}$  ratio ( $r$ ) = 2.2 and aging at 333 K for 16 h. (A)  $^{71}\text{Ga}$  NMR spectrum. (B)  $^{27}\text{Al}$  NMR spectrum.

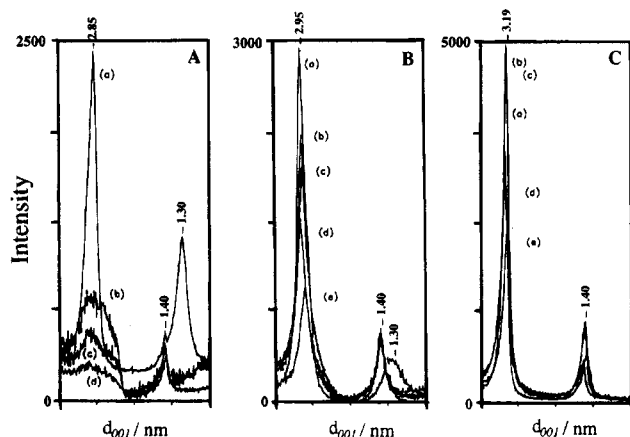


**Figure 2.** X-ray diffraction patterns of  $\text{GaAl}_{12}$ -pillared rectorites after calcination for 2 h in air at increasing temperatures. Displayed from 4.5 to 0.9 nm ( $2-10^\circ 2\theta$ ). (A)  $\text{GaAl-R2}$ . (B)  $\text{GaAl-R4}$ . (C)  $\text{GaAl-R6}$ . (a) 298 K; (b) 473 K; (c) 673 K; (d) 773 K; (e) 973 K.

caused the pillared structure to begin to collapse, with the sharp room temperature  $d_{001}$  reflection at 2.85 nm, corresponding to a gallery height of 0.95 nm, collapsing to a broad, low intensity peak centered around 2.65 nm (0.75 nm). The intensity of this broad signal was reduced further upon additional heating, until after calcination at 973 K, no further  $d_{001}$  signal was detected.

**Table 1. Physicochemical Properties of  $\text{GaAl}_{12}$ -Pillared Rectorites as Functions of Calcination Temperatures**

PILC sample	gallery height <sup>a</sup> (nm)					surface area <sup>b</sup> ( $\text{m}^2 \text{g}^{-1}$ )	
	298 K	473 K	673 K	773 K	973 K	423 K	773 K
GaAl-R2	0.95	0.75	0.70	0.70	n.o. <sup>c</sup>	156	88
GaAl-R4	1.05	0.99	0.96	0.93	0.89	225	165
GaAl-R6	1.29	1.20	1.20	1.05	1.00	394	322

<sup>a</sup> Calcined for 2 h in air. <sup>b</sup> Degassed at 423 K for 16 h. <sup>c</sup> Not observed.

This indicated either a loss of integrity of the sample slide, or formation of an amorphous aluminosilicate phase, most likely the former. A reflection observed at approximately 1.40 nm is ascribed to the second order  $d_{002}$  reflection of the basal spacing. The third reflection at approximately 1.30 nm, is assigned to the basal spacing of the nonpillared  $\text{Na}^+$ -exchanged smectitic layers. This reflection became weak and moved to approximately 0.95 nm after heating, confirming dehydration and collapse of the  $\text{Na}^+$ -exchanged swelling layers and, hence, this assignment. The results therefore indicate that intercalation of 2.0 mmol of  $\text{GaAl}_{12}$  pillaring solution  $\text{g}^{-1}$  of clay is insufficient to intercalate all the swelling layers<sup>5</sup> available in  $\text{Na}$ -rectorite. This creates a situation where the distance between pillars is greater than is required to maintain structural integrity of the pillared structure, leading to structural collapse at moderate calcination temperatures.

The XRD patterns of  $\text{GaAl-R4}$  under identical conditions (Figure 2B) show that the pillared structure of this material resisted thermal collapse considerably better than  $\text{GaAl-R2}$ . The basal spacings were larger than for  $\text{GaAl-R2}$  (Table 1), and the strong intensities of the  $d_{001}$  reflections suggest that the material was moderately well ordered. The increase in the concentration of pillaring molecules accounts for the considerably lower intensity of the reflection assigned to the unpillared clay, here observed as a shoulder on the  $d_{002}$  reflection. The pillared structure of  $\text{GaAl-R4}$  was preserved after calcination at elevated temperatures, with the gallery height falling only 15% from 1.05 to 0.89 nm after heating at 973 K for 2 h in air (Figure 2B(e)). The crystallographic order of the material, as indicated by the increasing width and decreasing intensity of the  $d_{001}$  reflection, was steadily reduced as the calcination temperature was increased. Significant pillared, and hence porous structure appeared however to be retained after treatment at this extreme (973 K) temperature.

In sharp contrast to the results obtained for  $\text{GaAl-R2}$  and improving further on the thermal stability displayed by  $\text{GaAl-R4}$ , the XRD patterns for  $\text{GaAl-R6}$  indicated that this material is both highly ordered and extremely stable to calcination in air (Figure 2C). No reflections due to unpillared smectite layers were observed, verifying that at a pillar concentration of 6.0 mmol of  $\text{GaAl}_{12}$   $\text{g}^{-1}$  clay, all of the swelling layers had been intercalated with  $\text{GaAl}_{12}$  cations. While the gallery height of  $\text{GaAl-R6}$  decreased from 1.25 to 1.20 nm after heating at 473 K (Figure 2C(b)) owing to dehydration of the pillars, the intensity of the  $d_{001}$  reflection actually increased. This suggested that removal of the interlayer and interparticle water increased the long range ordering of the pillared structure. The intensity of the  $d_{001}$  reflection was subsequently degraded slightly as the

calcination temperature was increased. After calcination at 973 K (Figure 2C(e)), the peak intensity was reduced to only approximately 50% of that of the most intense signal (Figure 2C(b)). The gallery height after calcination at this temperature was also intact, being only reduced to 1.00 nm.

**Surface Area Analysis.**  $\text{N}_2$  adsorption/desorption isotherms of the three materials displayed classic type I isotherms that are indicative of microporous materials having layered morphology. The BET surface areas calculated from the adsorption isotherms of PILCs calcined at 423 and 773 K are presented in Table 1. As was observed in recent reports,<sup>5,6</sup> the surface areas of pillared rectorites are lower, per gram of material, than those produced by  $\text{Al}_{13}$ - and  $\text{GaAl}_{12}$ -pillared montmorillonites. This is explained by the fact that there are fewer swelling exchange layers per unit mass of rectorite than montmorillonite. The surface areas of  $\text{GaAl}$ -R4 and  $\text{GaAl}$ -R6 are maintained after calcination at 773 K (Table 1), further indicating that these materials resisted both sintering and thermal degradation of the pillar species.

**Surface Acidity Characterization.** The IR spectra of adsorbed pyridine were used to investigate the surface acid characteristics of the three  $\text{GaAl}_{12}$  rectorites after activation at 773 K. Four modes arising from vibrations of the aromatic ring have been shown to be highly sensitive to the coordination environment and hence electron distribution of the pyridine molecule.<sup>12</sup> These modes and band position are assigned for liquid pyridine using the notation of Corrsin et al.,<sup>18</sup> as the  $\nu_{8a}$  ( $1580\text{ cm}^{-1}$ ),  $\nu_{8b}$  ( $1572\text{ cm}^{-1}$ ),  $\nu_{19a}$  ( $1482\text{ cm}^{-1}$ ), and  $\nu_{19b}$  ( $1439\text{ cm}^{-1}$ ) modes. The results obtained show agreement with earlier studies on the surface acidity of  $\text{Al}_{13}$ - and  $\text{GaAl}_{12}$ -pillared montmorillonites<sup>1,5,7</sup> and  $\text{Al}_{13}$ -pillared rectorite,<sup>4,5</sup> that while the surface acidity of PILCs is primarily of the Lewis type, considerable Brönsted acidity is also present.

Activation of the PILC samples at 773 K, removed all the surface adsorbed and H-bonded water from the PILC surface allowing the pyridine probe species to access all the possible surface sites. The dominant features in the spectra were similar for all three  $\text{GaAl}_{12}$  PILC samples only differing in relative intensities, therefore only the spectra of the most acidic material,  $\text{GaAl}$ -R6, will be discussed here (Figure 3). After evacuation of the excess pyridine vapor and physisorbed pyridine at 298 K, strong bands assigned to H-bonded pyridine were observed at 1426, 1452, and  $1614\text{ cm}^{-1}$ . These bands were accompanied by strong bands due to Brönsted pyridine at 1491 (19a), 1545 (19b), and  $1640\text{ cm}^{-1}$  (8b) and strong Lewis pyridine modes at 1452 (19b), 1491 (19a), and  $1620\text{ cm}^{-1}$  (8a), including a weak (8b) modes at  $1575\text{ cm}^{-1}$  (Figure 3a). As the desorption temperature was increased, the intensities of the various bands decreased with the H-bonded Brönsted pyridine bands being reduced to weak shoulders after evacuation of the sample at 373 K. Note, however, that the  $1452\text{ cm}^{-1}$  band maintained significant intensity after desorption at 373 K suggesting that it was produced by not only H-bonded pyridine but also possibly a second type of Lewis site. Increasing the temperature of evacuation to 473 K removed the bands

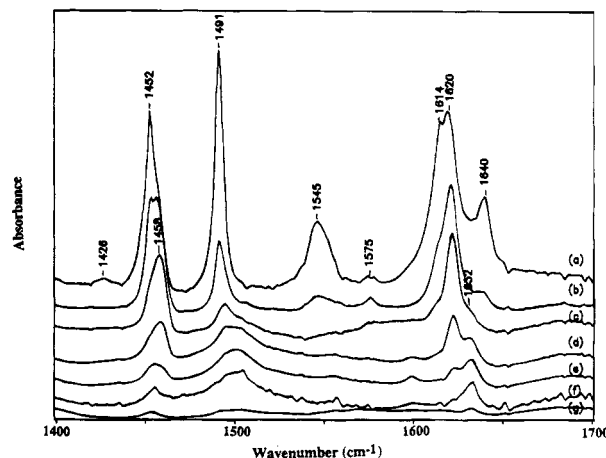


**Figure 3.** IR spectra of pyridine adsorbed on  $\text{GaAl}$ -R6 activated at 773 K, after desorption for 2 h at increasing temperatures. (a) 298 K; (b) 373 K; (c) 473 K; (d) 573 K; (e) 673 K; (f) 773 K; (g) 873 K.

due to adsorbed pyridinium and caused the intensities of the  $1452$  and  $1614\text{ cm}^{-1}$  bands to decrease further. At this same temperature, bands assigned to Lewis pyridine at  $1458$  and  $1620\text{ cm}^{-1}$  appeared to maintain their intensities. The intensity of the  $1491\text{ cm}^{-1}$  B + L 19a mode decreased significantly as the bands due to Brönsted pyridine were removed. It is a mistake to equate desorption of adsorbed pyridinium bands with removal of the Brönsted acidity itself. If pyridine is readsorbed, the same pyridinium bands will be regenerated, indicating that the proton sites have not been destroyed, simply that the adsorbate has been removed.

Note that as the desorption temperature increased to 573 K (Figure 3d) a second 19a mode appeared at  $1498\text{ cm}^{-1}$  and the  $1452\text{ cm}^{-1}$  band shifted to  $1455\text{ cm}^{-1}$ . After desorption at 473 K, a shoulder appeared at  $1632\text{ cm}^{-1}$ . The intensity of this band was maintained as the intensity of the  $1620\text{ cm}^{-1}$  band decreased. As the temperature of desorption was increased further, the intensities of the remaining bands in the spectrum steadily decreased, until after heating of the sample at 873 K a trace of the adsorbate still persisted. Note again, that removal of the adsorbate does not equate to the removal of the acid site. Under conditions where poisoning is not a complication, the Lewis acid sites will persist until the temperature is reached where the structure of the material being studied undergoes a phase transition and is thereby destroyed.

The coincident B + L 19a mode exhibited interesting behavior. Initially the band was sharp and intense at  $1491\text{ cm}^{-1}$ . After heating the band was reduced to a weak and broad doublet indicative of two separate components at 1491 and  $1498\text{ cm}^{-1}$ . The former component is assigned to the Brönsted pyridine contributor, while the latter is assigned to the Lewis pyridine component. If one analyzes the area under the  $1545\text{ cm}^{-1}$  (8b) pyridinium band at 298 K, it can be ascertained that the concentration of surface pyridinium is comparable to that of coordinated pyridine. Behavior suggestive of two different surface Lewis acid sites was observed in the bands assigned to Lewis pyridine. The bands at  $1455$ ,  $1458$ ,  $1620$ , and  $1632\text{ cm}^{-1}$  persisted to high desorption temperatures allowing assignment of all four bands to Lewis pyridine. This group of bands may be divided into pairs,  $1458/1620\text{ cm}^{-1}$  and  $1455/$

(18) Corrsin, L.; Fax, B. S.; Lord, R. C. *J. Chem. Phys.* **1953**, *21*, 1170.

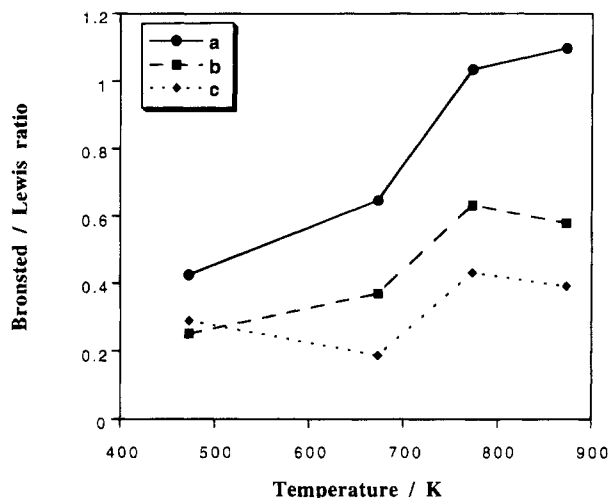


**Figure 4.** Brønsted/Lewis acid site ratios calculated from the surface area corrected intensities of the  $1545\text{ cm}^{-1}$  pyridinium band and the  $1452\text{ cm}^{-1}$  Lewis pyridine band after evacuation of the samples at 373 K. No correction for relative molar absorptivities is applied owing to the disagreements in the literature regarding these values (see text). (a) GaAl-R2; (b) GaAl-R4; (c) GaAl-R6.

$1632\text{ cm}^{-1}$ , where the former, less widely separated pair is assigned to pyridine coordinated to weaker Lewis acid sites and the latter, more separated pair, to stronger surface sites.

We propose that this observation is consistent with the conclusions reported by Bradley et al.<sup>19</sup> that the contribution made to the surface Lewis acidity by the smectite layers is significant. The individual contributions made by the exposed clay layers and the pillar surfaces can be differentiated by careful analysis of the IR spectra of adsorbed pyridine. In the current study we assert that the weaker Lewis acid sites are found on the exposed clay layers, while the stronger Lewis acid sites are found on the surfaces of the pillars. There is very little agreement in the literature regarding values for the molar absorptivities of the vibrational modes of adsorbed pyridine.<sup>20–22</sup> In fact, it is the opinion of the authors that such values are dependent upon the particular adsorbent, the surface site and surface population of the system under investigation. As a result therefore, only relative values and the trends displayed therein may be discussed. Figure 4 presents the relative Brønsted/Lewis acid site ratios of GaAl-R2, 4 and 6 after calcination at temperatures ranging from 473 to 873 K. The B/L ratios are calculated from the absorbance values of the  $1452$  and  $1545\text{ cm}^{-1}$  L and B pyridine bands after evacuation of the sample at 373 K. These data indicate that as the pillar loading is increased, the concentration of Lewis acid sites increases at a rate greater than that of the Brønsted acid sites. This is exhibited in the plots which show B/L ratios  $\text{GaAl-R2} > \text{GaAl-R4} > \text{GaAl-R6}$  and indicates that the number of Lewis acid sites produced per pillar is greater than the number of Brønsted acid sites. Increasing the calcination temperature increases the B/L ratios of all three PILCs. This can be explained by

either, increased production of acidic surface OH groups by the dehydration of the structure that occurs as the calcination temperature is increased or greater contribution of clay OH groups as the PILC structure collapses. As the thermal stability of the PILC structure increases, the Lewis acid sites become more stable and degrade at a lower rate than the Brønsted acid sites. This is exhibited by the smaller difference in B/L ratios after calcination at 473 and 873 K of GaAl-R6 over GaAl-R2.

Several authors<sup>1–3,23,24</sup> have reported that the existence of Brønsted acidity on PILC surfaces can be explained by a single mechanism. This mechanism proposes that upon calcination of a polyoxo oligomer-exchanged clay, an  $\text{MO}_4$  tetrahedron in the tetrahedral layer of the host clay adjacent to the pillar cation undergoes inversion and cross-linking to an apex of the cation. Protons are supplied by the dehydroxylation and hydrolysis of the oligocation causing the pillar-O-M (where M = Al, Si, Mg,  $\text{Fe}^{\text{III}}$ ) linkage to be protonated at the oxygen atom, thereby producing an acidic hydroxyl site. The acid strengths of these protons would be expected to be high, owing to the strained nature of this pillar-layer cross-link. There is little evidence to show that  $\text{Al}_{13}$  or  $\text{GaAl}_{12}$  oligocations form pillars with distinct crystal structures other than possibly  $\gamma$ -alumina;<sup>23</sup> therefore, it seems likely that on a nanoscopic scale such as that involved here, that it is not possible to assign a distinct crystallographic form to the pillars. The surfaces of the individual alumina pillars are unlikely, therefore, to contribute strongly to the Brønsted acidity. The second source of protonic acidity arises from the exposed surfaces of the phyllosilicate layers at platelet fractures, defects and edges where the octahedral layers and hence Al-OH groups are exposed. We propose that such contributions to the Brønsted acidity of PILC materials are significant.

## Conclusions

The narrow, high-intensity XRD reflections after heating indicate that intercalation of  $\text{GaAl}_{12}$  oligocations into the interlayer space of rectorite produces a pillared structure that is highly ordered and more thermally stable than those reported to date for  $\text{GaAl}_{12}$ -pillared montmorillonite. One cannot, however, assume that this material possesses greater hydrothermal stability than that observed for  $\text{Al}_{13}$ -pillared rectorite until steaming experiments are conducted. The results confirm that as the concentration of pillaring species is increased, the thermal stability of the pillared structure increases. There will be a critical concentration at which no more pillaring material can be incorporated without the formation of "extraframework" metal oxide phases. This value is related to the cation exchange concentration of the parent clay and can be increased by specific treatments.<sup>9</sup> The strength and population of both the Lewis and Brønsted acidity and hence the Brønsted/Lewis ratios can be tuned by varying the concentration of pillars incorporated into the layered host structure. Careful examination of the IR spectra of adsorbed pyridine allows differentiation of two dif-

(19) Bradley, S. M.; Kydd, R. A. *J. Catal.* **1993**, *141*, 239.

(20) Hughes, T. R.; White, H. M. *J. Phys. Chem.* **1967**, *71*, 2192.

(21) LeFrancis, M.; Malbois, G. *J. Catal.* **1971**, *20*, 350.

(22) Sayed, M. B.; Kydd, R. A.; Cooney, R. P. *J. Catal.* **1984**, *88*, 137.

(23) Tennakoon, D. T. B.; Jones, W.; Thomas, J. M. *J. Chem. Soc., Faraday Trans. 1* **1988**, *86*, 3081.

(24) Zeng, L.; Hao, Y.; Tao, L.; Zhang, Y.; Xue, Z. *Zeolites* **1991**, *12*, 374.

ferent types of surface Lewis acid site. The weaker site is found on the exposed clay layers, while the stronger site is found on the surface of the introduced pillars.

While rectorite is considerably less abundant than montmorillonite, vast deposits occur in regions of China, and it has proven to be very beneficial to the preparation of PILCs with superior properties. We propose that the use of clays such as rectorite, which possesses isomorphous substitution in the tetrahedral layers and interstratified "double-layer" structures, inhibit sintering of the pillars at high temperature by the formation of strong pillar-layer cross links at the sites of tetrahedral substitution and collapse of the layered structure owing

to the lower flexibility of the layers in the interstratified structure and greater resistance to chemical degradation.

**Acknowledgment.** This work was partially funded by the donors of Petroleum Research Fund of the American Chemical Society (Grant No. 20174-AC5). S.A.B thanks the New Zealand Ministry of Research, Science and Technology for a postgraduate study award for New Zealand Maori students of Science and Engineering.

CM950069J